Analysis of Texture and Microstructure of Annealed Fe–23Mn–3Si–3Al Steel

J. Kowalska[*]

AGH University of Science and Technology, Faculty of Metals Engineering and Industrial Computer Science,
Cracow, Poland

Texture and microstructural examinations of Fe–23%Mn–3%Si–3%Al (mass%) alloy are presented. After casting the ingot was homogenized at 1150 °C, hot-rolled in the temperature range 1200 °C-900 °C and then cold-rolled. Steel samples, after 40% deformation, were annealed at 300 °C for 10 min, 600 °C and 750 °C for 30 min. X-ray diffraction and metallographic studies revealed deformation-induced mechanical twinning and phase transformation. The crystallographic Shoji–Nishiyama and Kurdjumov–Sachs relations between martensite (ε, α') and austenite (γ), were found in the cold-rolled material. During annealing the reverse martensite to austenite transformation occurred.

1. Introduction

In the recent decades, a substantial interest has been attracted by high-manganese steels. They possess very good functional properties as far as combination of strength and plasticity is concerned [1]. In these alloys, plastic deformation may take place by twinning (the TWIP effect — twinning induced plasticity) or a martensitic transformation induced by deformation (the TRIP effect — transformation induced plasticity) [1–6]. In numerous cases both of those effects may occur simultaneously. That, in turn, is dependent upon the chemical composition and the temperature of deformation. It had been presumed that if the content of a manganese in a steel does not reach 15 mass percent, it manifests the TRIP effect, and between 15 a 25%, TRIP and TWIP effects are observed. In turn, when the quantity of manganese in a steel is higher than 25%, then the dominant mechanism of deformation is twinning [4]. Temperature exerts a substantial influence upon stacking fault energy, and, as a result, the stability of austenite. Simultaneously with decrease in temperature, decrease in the value of stacking-fault energy is observed, which is conducive to martensitic transformation [7].

There is a close correlation between factors determining the formation and the development of deformation texture and stacking-fault energy. The development of the texture in the course of deformation and annealing is very important because it determines mechanical properties, which, in turn, define the suitability of a steel for industrial applications.

In this paper, the subject matter of the analysis is the results of the research conducted into the Fe–23Mn–3Si–3Al high-manganese steel, in which in the course of cold

plastic deformation, there occurs both martensitic transformation induced by deformation, and also mechanical twinning alike. In turn, in the course of annealing the deformed steel, there occurred the reverse transformation of martensite into austenite.

2. Material and methods

The 22.96% manganese, 2.85% silicon, 2.66% aluminium and 0.065% carbon steel was cast in a vacuum induction furnace. After casting, the ingot was subjected to homogenization at 1150 °C and hot rolling from the starting temperature of 1200 °C. The material was then subjected to cold deformation by laboratory rolling to 40%. The steel was subsequently annealed at 300 °C for 10 min, at 600 °C for 30 min, 750 °C for 30 min, and cooled in air.

Samples for the diffraction research were ground on abrasive papers, polished by diamond pastes and, subsequently, electrically polished. For the purpose of the X-ray examinations, the following diffractometers: Bruker D8 Advance, Siemens D500 and D5000 were used (Co K_α, Cu K_α and Mo K_α radiation, respectively). Diffraction research included qualitative phase analysis and the measurement of a crystallographic texture.

Samples for metallographic research were taken from the longitudinal section of a sheet. The observations of the microstructure were performed on a JEM 200CX transmission electron microscope.

3. Results and discussion

The diffractogram presented in Fig. 1 for the initial state of the Fe–23Mn–3Si–3Al alloy shows that the steel possesses a single-phase austenitic (γ) structure. On the diffractogram of the samples after 20% deformation (Fig. 1), apart from peaks, originating from austenite (γ), there appear additional diffraction lines from martensite

---

[*]corresponding author; e-mail: joannak@agh.edu.pl

ε and α' ((101)ε, (103)ε, (110)α', (200)α' and (211)α'). Simultaneously with increase in deformation, reaching 40%, further changes in the diffraction image are observed. The peaks originating from martensite ε are not present, whereas there increases the intensity of the lines originating from martensite α' (Fig. 1). This indicates that martensitic transformation induced by deformation occurs in the following manner: $\gamma \to \varepsilon$ and $\varepsilon \to \alpha'$. It was not possible to detect by X-ray methods the remaining amount of martensite ε at this stage of deformation. In the diffraction image pattern of the sample after annealing at 300 °C, the intensity of peaks originating from the phases: γ and α' increases, which is caused by recovery processes. Simultaneously with increase in the temperature of annealing, it is possible to observe the decrease in the intensity of peaks originating from martensite α'. After annealing at 750 °C, only the lines originating from a single phase of austenite γ are present on the diffractogram (Fig. 1). This is evidence that a reverse transformation $\alpha' \to \gamma$ has occurred. Data in the literature [8] state that reverse transformation $\varepsilon \to \gamma$ occurs at temperatures of 100 °C–250 °C, whereas the transformation $\alpha' \to \gamma$ is in the temperature range 500 °C–700 °C.

Fig. 2. Orientation distribution functions in sections $\phi_2$const for austenite (a) in the initial state, (b) after 20% cold-rolling, (c) after 40% cold-rolling, (d-f) after 40% cold-rolling and annealing at 300 °C, 600 °C and 750 °C, respectively.
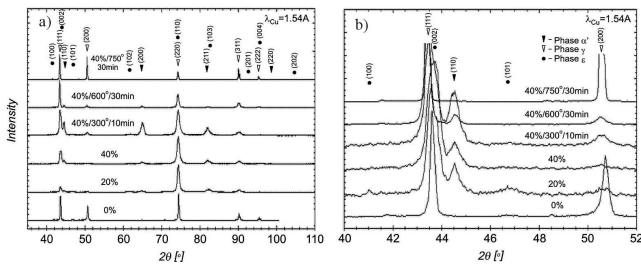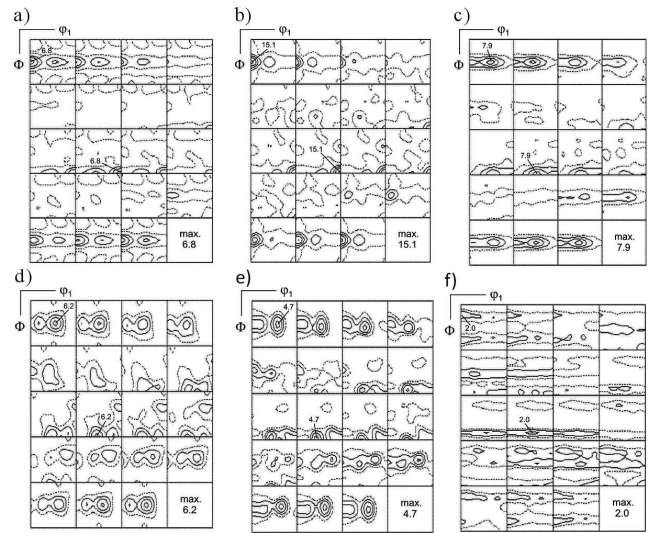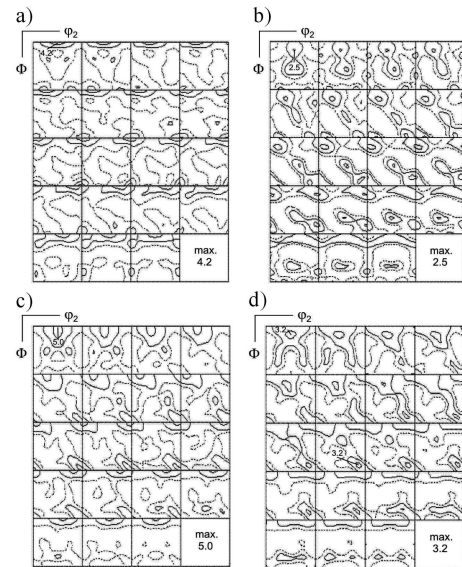

Fig. 1. X-ray diffractions patterns of the Fe-23Mn-3Si-3Al alloy, (a) in the initial state (0%), after 20% and 40% cold-rolling, and after annealing at 300 °C, 600 °C and 750 °C, (b) the expanded plot of the (111) and (200) for austenite and the (002) and (101) for martensite ε peaks (b).

The analysis of a crystallographic texture was conducted upon the basis of orientation distribution function (ODF)ODF and the selected full pole figures (Figs. 2–4).

Austenite in the initial sample possesses a comparatively strong texture, and the maximum was compatible with the Goss orientation {110}⟨001⟩. The main texture components of austenite are related to the fibre $\alpha = \langle 110 \rangle \| ND$ (normal direction) (Fig. 2a). The texture indexes of austenite increase after 20% of deformation. The maximum value of ODF $f(g) = 15.1$ is compatible with the Goss orientation. In the texture (Fig. 2b), a weak orientation {113}⟨332⟩ was observable. After 40% deformation, the degree of the texturization of austenite decreases, which is connected with the phase transformation $\gamma \to \varepsilon \to \alpha'$ (Fig. 2c). The disappearance of the component {112}⟨111⟩ was observed. This is evidence for the occurrence of mechanical twinning. This lack of that orientation may be connected with, that in

Fig. 3. Orientation distribution functions in sections $\varphi_1 = $ const for martensite α' after (a) 20% cold-rolling, (b) 40% cold-rolling, (c, d) 40% cold-rolling and annealing at 300 °C and 600 °C, respectively.
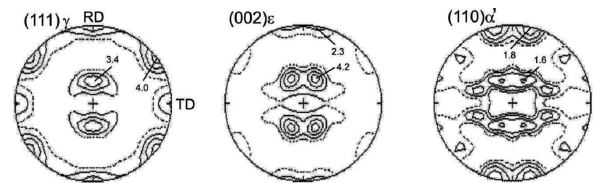

Fig. 4. Calculated pole figure for austenite (111)γ, for hexagonal martensite (002)ε and for regular martensite (110)α'- sample after 20% cold-rolling. (RD — rolling direction, TD — trasnsverse direction).

accordance with the Kurdjumov–Sachs relationship, it is becoming to the orientation $\{112\}\langle110\rangle$ of martensite [9]. The maximum of ODF is compatible with the orientation $\{110\}\langle557\rangle$ (Fig. 2c). The texture of austenite after deformation tends to become a texture of alloy type. This is a typical orientation in the metals and alloys which have a regular structure with low level of stacking-fault energy.

After annealing at 300 °C, the texture of austenite is relatively weak. The $\alpha = \langle110\rangle\|ND$ fibre undergoes shortening, and stretched from the orientation $\{110\}\langle001\rangle$ to $\{110\}\langle447\rangle$. In the texture, it is still possible to observe a weak component $\{113\}\langle332\rangle$, and there occurs the S type orientation $\{123\}\langle364\rangle$ (Fig. 2d). Annealing at 600 °C causes changes in the texture, and the degree of texturization decreases. Weakening is observed in the orientation $\{110\}\langle112\rangle$ and the component $\{113\}\langle332\rangle$ disappears (Fig. 2e).

Annealing at 750 °C results in clear weakening of the texture. Orientations in the $\alpha = \langle110\rangle\|ND$ fibre disappear. It is possible to observe two restricted weak fibres $\{013\}\langle uvw\rangle$, having the strongest orientation $\{013\}\langle100\rangle$. That is connected with the occurring of recrystallization processes (Fig. 2f). Even though a typical component occurring in the texture of recrystallized austenite is a cubic orientation $\{100\}\langle001\rangle$, regardless of that, in the case of this steel, that orientation is absent. Similar results were reported in the paper of Escobar and collaborators [8].

The texture of martensite α' after deformation is comparatively weak. The maximum value of ODF is within the fibre $\alpha_1 = \langle110\rangle\|RD$ and is compatible with the orientation $\{100\}\langle011\rangle$–20% deformation and the component $\approx \{311\}\langle011\rangle$–40% deformation (Fig. 3a and b). In the material after 20% deformation, orientations found in the fibre: $\varepsilon = \langle001\rangle\|ND$ (Fig. 3a) became noticeable in the texture as well.

After annealing at 300 °C, the texture becomes more acute, which is connected with the recovery processes occurring (Fig. 3c). After annealing at 600 °C, the degree of texturization decreases. In this temperature range, there occurs a reverse transformation $\alpha' \rightarrow \gamma$. Texture of martensite α' becomes random, still manifesting a fibrous character. In the texture, there occur weak orientations found in the fibres $\alpha_1 = \langle110\rangle\|RD$ and $\varepsilon = \langle001\rangle\|ND$ (Fig. 3d).

In Fig. 4, the pole figures $(111)\gamma$, $(002)\varepsilon$ and $(110)\alpha'$ for samples after 20% deformation are presented. It was ascertained that there occur crystallographic correlations between austenite (γ) and martensite (ε and α'). The relation between the phases γ and ε is referred to as the Shoji–Nishiyama relationship (S–N) $\{002\}\varepsilon\|\{111\}\gamma$ and $\langle110\rangle\varepsilon\|\langle110\rangle\gamma$ [10]. Such a correlation was reported also in other papers devoted to high-manganese steels [5, 6, 11].

The relation between certain orientations of austenite and martensite α' is described by the Kurdjumov–Sachs relationship (K–S) $\{111\}\gamma\|\{101\}\alpha'$ and $\langle101\rangle\gamma\|\langle111\rangle\alpha'$. It is possible to observe that not all the variants are being conducted, and that the transformations: $\gamma \rightarrow \varepsilon$ and $\gamma \rightarrow \alpha'$ occur with the variant selection (Fig. 4).

The microstructure of the steel after different degrees of plastic deformation was discussed in detail in Ref. [12] and this article only shows the microstructure after 40% deformation.

Then micro-deformation twins and martensite α', are observable (Fig. 5a and b). After annealing at 300 °C, bands are observed in the microstructure and in these bands new crystallites of austenite are formed.
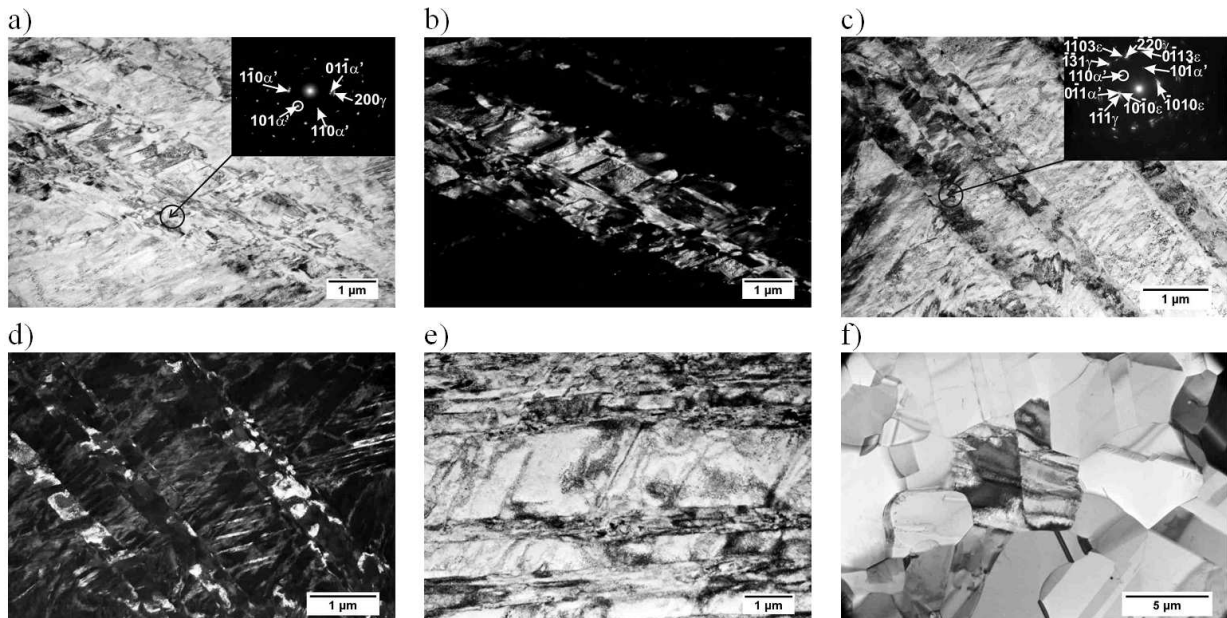

Fig. 5. TEM micrographs of Fe-23Mn-3Si-3Al alloy: (a-b) after 40% cold-rolling, bright field (BF) diffraction pattern $[\bar{1}11]\alpha'$ and dark field (DF) with $(101)\alpha'$ after 40% cold-rolling and annealing: (c-d) 300 °C for 10 minutes, BF diffraction pattern $[\bar{1}12]\gamma\|[\bar{1}11]\alpha'\|[12\bar{1}1]\varepsilon$ and DF with $(110)\alpha'$, (e) 600 °C for 30 minutes, BF, (f) 750 °C for 30 minutes, BF.

Data in the literature indicate that in this temperature range there occurs the following transformation: $\varepsilon \to \gamma$ [8]. In the structure, apart from austenite, the martensite (ε and α') are present, which is observable by selective diffraction. Dark field observation shows that martensite α' it is situated principally in shear bands (Fig. 5c and d). In the sample annealed at 600 °C, the band character of the microstructure is maintained (Fig. 5e). After annealing at 750 °C, recrystallization of austenite occurs, but regardless of that, there are very few observable areas which are not crystallized (Fig. 5f).

4. Summary

Analysis of the texture and the microstructure of the Fe-23Mn-3Si-3Al metastable steel is complex, because in the course of cold plastic deformation there simultaneously occur deformation of austenite, phase transformation induced by deformation: $\gamma \to \varepsilon \to \alpha'$ and deformation of martensite formed at a given stage of plastic working. In the course of annealing this steel, the reverse transformation $\varepsilon \to \gamma$ and $\alpha' \to \gamma$ occurred. After annealing the texture of austenite underwent weakening, which is connected with occurring recrystallization processes.

Acknowledgments

References

[1] O. Grässel, G. Frommeyer, C. Derder, H. Hofmann, *J. Phys. IV* **110**, 383 (1997).

[2] S. Alain, J.-P. Chateau, O. Bouaziz, S. Migot, N. Guelton, *Mater. Sci. Eng. A* **387-389**, 158 (2004).

[3] Y.F. Shen, C.H. Qui, L. Wang, X. Sun, X.M. Zhao, L. Zuo, *Mater. Sci. Eng. A* **561**, 329 (2013).

[4] H. Ding, H. Ding, D. Song, Z. Tang, P. Yang, *Mater. Sci. Eng. A* **528**, 868 (2011).

[5] J. Kowalska, W. Ratuszek, M. Witkowska, A. Zielińska-Lipiec, T. Tokarski, *J. Alloys Comp.* **643**, S39 (2015).

[6] J. Kowalska, W. Ratuszek, M. Witkowska, A. Zielińska-Lipiec, *J. Alloys Comp.* **615**, S583 (2014).

[7] M. Koyama, T. Sawaguchi, T. Lee, C.S. Lee, K. Tsuzaki, *Mater. Sci. Eng. A* **528**, 7310 (2011).

[8] D.P. Escobar, S.S. Ferreira de Dafé, D.B. Santos, *J. Mater. Res. Technol.* **4**, 162 (2015).

[9] S.G. Chowdhury, S. Das, P.K. De, *Acta Mater.* **53**, 3951 (2005).

[10] W. Zhang, Z. Liu, Z. Zhan, G. Wang, *Mater. Lett.* **91**, 158 (2013).

[11] Y. Lü, B. Hutchinson, D.A. Molodov, G. Gottsrein, *Acta Mater.* **58**, 3079 (2010).

[12] J. Kowalska, W. Ratuszek, M. Witkowska, A. Zielińska-Lipiec, M. Kowalska, *Arch. Metall. Mater.* **60**, 1789 (2015).